FUEL CONVERSION EFFECT ON NEUTRONICS PERFORMANCE OF YALINA-BOOSTER SUB-CRITICAL ASSEMBLY FROM HEU TO LEU

H. KIYAVITSKYA, YU. FOKOV, V. BOURNOS, S. MAZANIK, CH. ROUTKOVSKAYA, S. SADOVICH
JIPNR-Sosny,
National Academy of Sciences of Belarus,
Minsk,
Belarus

Y. GOHAR
Argonne National Laboratory,
Argonne, IL,
USA

I. BOLSHINSKI
Idaho National Laboratory,
Idaho Falls, ID,
USA

Abstract

"YALINA-Booster" is a fast-thermal sub-critical facility intended for investigating the neutronics of accelerator driven systems (ADS) at different sub-criticality levels, different configurations, and fuel compositions for the ADS development. The conversion of the YALINA-Booster assembly with highly enriched uranium (HEU) fuel in fast zone (36 and 90% of ^{235}U) to the low enriched uranium (LEU) with ^{235}U of less than 20% without performance losses has been performed. The experimental research program have covered the measurements of sub-criticality levels, spatial distribution of neutron flux, time dependent neutron flux measurements from different neutron source pulse durations, threshold reaction rates, transmutation reaction rates, neutron spectrum, etc. One of the important issues is the validation of the current experimental methods and techniques and their adaptation for use in ADS experiments. In this paper, the main neutronics parameters of YALINA-Booster with HEU and LEU fuels are considered.

1. YALINA-BOOSTER SUB-CRITICAL ASSEMBLY DESIGN

YALINA-Booster is a zero power fast-thermal sub-critical assembly driven by an external neutron source. It consists of fast zone, thermal zone, interface absorber zone between the fast and thermal zones, radial and axial reflector zones. There is a hole in middle of the assembly with lead material for locating the neutron source. The assembly has square configuration consisting of 36 lead subassemblies in the fast zone and 108 polyethylene subassemblies in the thermal zone as shown in Fig. 1. The fast zone is subdivided to inner and outer parts. Depending on the configuration, the inner part can be loaded by $U_{met.}$ (90% ^{235}U enrichment), UO_2 (36% ^{235}U enrichment), or UO_2 (21% ^{235}U enrichment). The outer part of the fast zone can be loaded either by UO_2 (36% ^{235}U enrichment) or UO_2 (21%^{235}U enrichment). The interface zone surrounds the fast zone and it consists of inner layer of natural uranium rods and outer layer of boron carbide rods. It provides a one-directional coupling between the fast and the thermal zones, which prevents thermal neutrons from entering the fast zone.

The thermal zone surrounds the absorber zone. It consists of 108 polyethylene subassemblies and each subassembly has 16 fuel channels arranged in a 20 mm square lattice. The fuel rods have UO_2 with 10% ^{235}U enrichment.

There are 4 experimental channels in the fast zone (EC1B, EC2B, EC3B and EC4B), 3 experimental channels in the thermal zone (EC5T, EC6T, and EC7T), and 3 experimental

channels in the graphite reflector (EC8R, EC9R and EC10R). The channels are used for locating different detectors or material samples. There are 4 measurement channels in graphite reflector (MC1-MC4) to monitor neutron flux density. Two additional measurement channels are located in thermal zone (MC5 and MC6). In the axial direction, borated polyethylene is used as a reflector and biological shielding.

1.1 YALINA-Booster main configurations

In the course of the experimental program implementation a large number of configurations was examined. In this paper, the attention will be focused on three configurations:

1st configuration - HEU fuel YALINA-Booster - using 132 fuel rods with 90% ^{235}U enrichment U_{met} in the inner part of fast zone; 563 fuel rods with 36% ^{235}U enrichment UO_2 in the outer part of fast zone, and 1141 fuel rods (EK-10) with 10% ^{235}U enrichment UO_2 in thermal zone, ($k_{eff} \leq 0.979$);

2nd configuration - YALINA-Booster (1st step of conversion to LEU fuel) -with 695 fuel rods with 36% ^{235}U enrichment UO_2 in fast zone and 1185 fuel rods (EK-10) with 10% ^{235}U enrichment UO_2 in thermal zone ($k_{eff} \leq 0.975$);

3rd configuration - LEU fuel YALINA-Booster (2nd step of conversion to LEU fuel) with 601 fuel rods with 21% ^{235}U enrichment UO_2 in fast zone and 1185 fuel rods (EK-10) with 10% ^{235}U enrichment UO_2 in the thermal zone ($k_{eff} \leq 0.960$).

The complete description of the configurations is available at the IAEA website (http://www-nfcis.iaea.org/NFCIS).

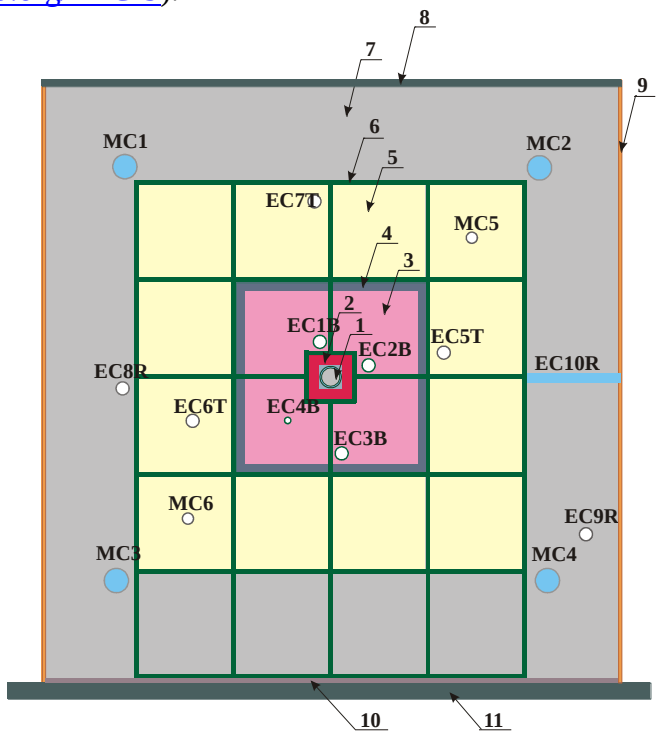

1 - Ionguide, 2 - inner fast zone, 3 - outer fast zone, 4 - absorber,
5 - thermal zone, 6 - SS frame, 7 - graphite reflector, 8 - upper plate,
9 - organic glass sheet, 10 - cadmium layer, 11 - bottom plate

FIG. 1. Cross section of YALINA-Booster assembly.

1.2 Equipment

The experimental measurements have been carried by small and long size ^{3}He-detectors and fission chambers with ^{235}U and ^{238}U sensitive areas. Pulsed Neutron Source (PNS) experiments have been carried out with application of time analyzer Turbo MCS and Data Acquisition Systems based on counter/timers PCI-6602 and PXI-6602.

2. NEUTRONICS PARAMETERS OF THE YALINA-BOOSTER FUELED BY HEU

A large number of experiments was performed as a function of ^{235}U mass to determine the sub-criticality values by different experimental techniques. The measured k_{eff} values as a function of ^{235}U mass using the reciprocal counting method during the fast zone fuel loading is presented in Fig. 2.

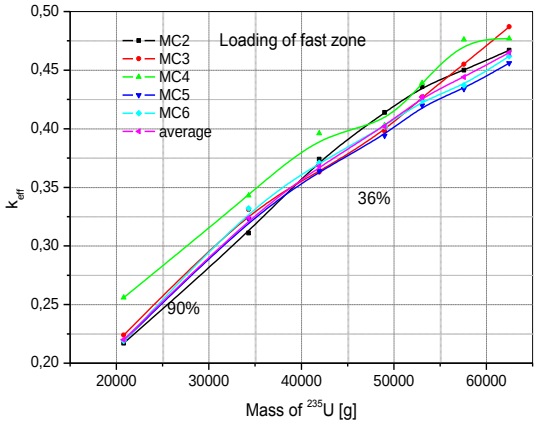

FIG. 2. Effective neutron multiplication factor measured by the reciprocal counting method during the fast zone fuel loading.

The fast fuel zone was loaded with 132 fuel rods with 90% enriched $U_{met.}$ in the inner part and 563 fuel rods with 36% enriched UO_2 in the outer part. Then the loading of thermal zone was started. To get more reliable results the PNS method was used along with the reciprocal counting method. The effective multiplication factors obtained by the two methods are compared in Fig. 3.

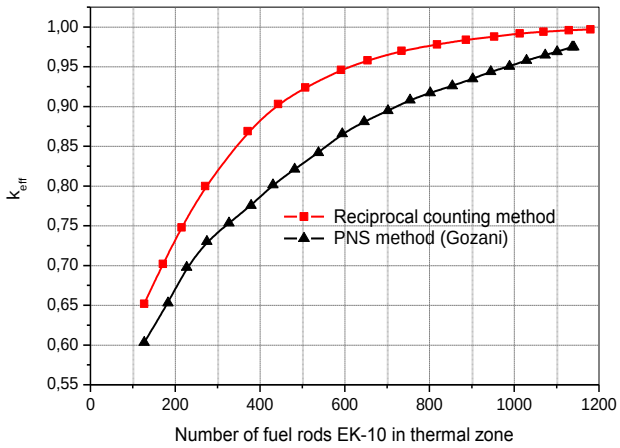

FIG. 3. Comparison of k_{eff} values measured by the PNS method and the reciprocal counting method during the thermal zone loading with EK-10 fuel rods.

The total number of EK-10 fuel rods in the thermal zone is 1141. For this configuration, the spatial and time distribution reaction rates have been measured by fission chambers KHT-

5 and KHT-8 in different experimental channels. Figs 4 shows the axial distribution of the fission reaction rate distribution in the experimental channels EC2B (a) and EC5T (b) measured by the fission chamber KHT-5 with DT neutron source and Fig. 5 shows the axial distribution of ^{238}U(n,f) reaction rates measured by the fission chamber KHT-8 in the experimental channel EC2B. The calculated axial distributions of the neutron flux density in experimental channels EC2B (a) and EC5T (b) with MCNP from D-T neutron source are shown in in Fig. 6.

The increase of the neutron flux density near the ends of fuel rods in fast zone shown in Fig. 6(a) is due to the low energy neutrons diffusing from the axial reflector. Such effect does not exist in the thermal zone as shown if Fig. 6 (b).

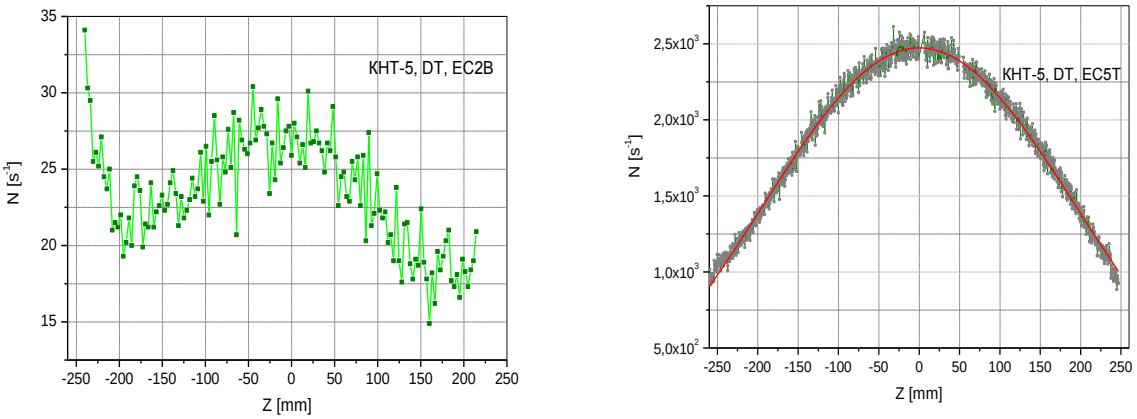

a b

FIG. 4. Axial distribution of the fission reaction rate in the experimental channels EC2B (a) and EC5T (b) measured by the fission chamber KHT-5 with DT neutron source.

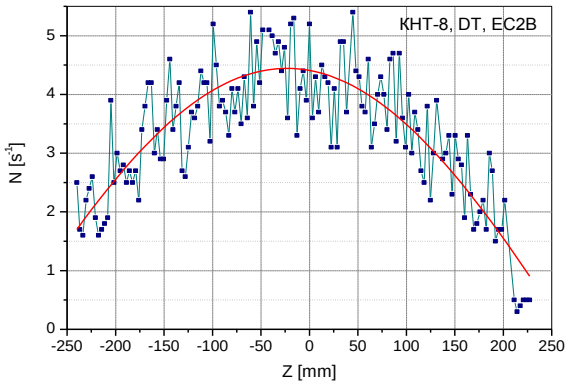

FIG. 5. Axial distribution of ^{238}U(n,f) reaction rates measured by the fission chamber KHT-8 in the experimental channel EC2B.

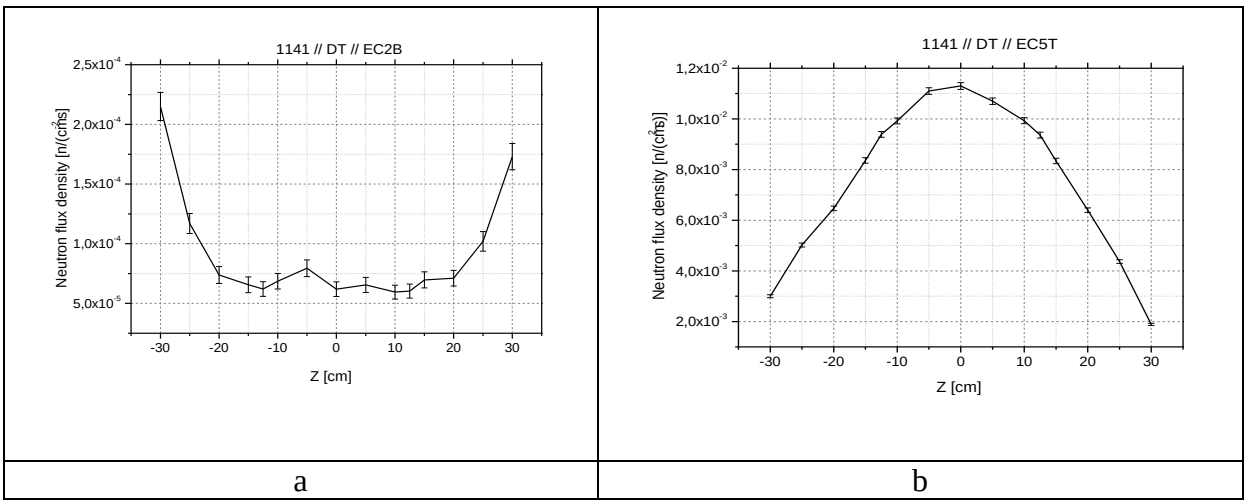

FIG. 6. Calculated axial distribution of the neutron flux density in experimental channels EC2B (a) and EC5T (b) with MCNP from D-T neutron source.

The time dependent Helium-3 reaction rates from 10 μs D-T neutron pulse measured in the different experimental channels are shown in Fig. 7. The reaction rate values in the thermal experimental channel exceed the possible pulse counting rate, which requires Cd wrapping of the detector to reduce the measured reaction rates. The experimental results show that it is better to use D-D neutron source for performing the measurements in the thermal experimental channels.

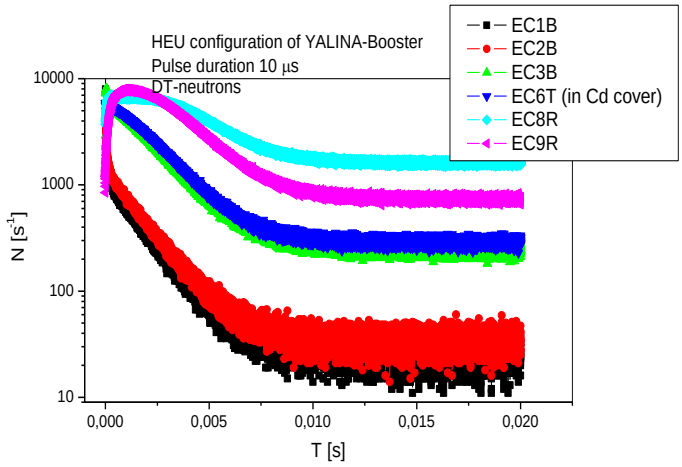

FIG. 7. Time dependent Helium-3 reaction rate from 10 μs D-T neutron pulse measured in the different experimental channels.

3. NEUTRONICS PARAMETERS OF THE YALINA-BOOSTER AT THE FIRST LEU CONVERSION STEP

In the first LEU conversion step, the 90% enriched U_{met} fuel rods were extracted from the inner part of the fast zone and replaced with 36% enriched UO_2 fuel rods. The total number of these fuel rods in fast zone was 695 and the number of EK-10 fuel rods in thermal zone was 1141. The counting rates from the small ^{3}He-detectors located in MC5 and MC6 measurement channels are shown in Fig. 8 during the 36% enriched UO_2 fuel rods loading into the inner part of the fast. The green line marks the beginning of the loading procedure. The counting rate shows a small increase during the loading process, which indicates the low contribution of the inner part of the fast zone to the total reactivity of the assembly. To

increase k_{eff} to the original value, extra 44 EK-10 fuel rods were loaded into the thermal zone. The total number of the loaded EK-10 fuel rods was 1185. Therefore the second YALINA-Booster configuration contained 695 UO_2 fuel rods with 36% enriched uranium in fast zone and 1185 fuel rods EK-10 in thermal zone.

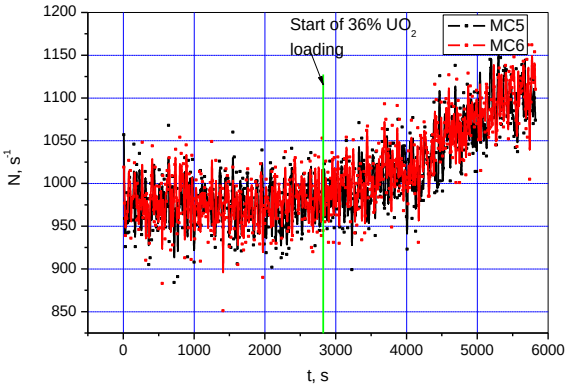

FIG. 8. Variation of ^{3}He detectors' counting rates during load of the 36% enriched UO_2 into the inner part of the fast zone.

The experimental k_{eff} values of the first and second configurations of YALINA-Booster as a function of the number of EK-10 fuel rods in thermal zone are presented in Fig. 9. The calculated k_{eff} values as a function of the loaded ^{235}U mass is shown in Fig. 10 simulating the fuel loading steps.

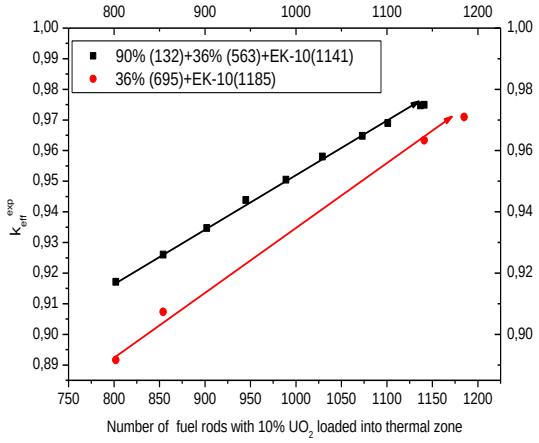

FIG. 9. Experimental k_{eff} values of the first and second configurations of YALINA-Booster as a function of the number of EK-10 fuel rods in thermal zone.

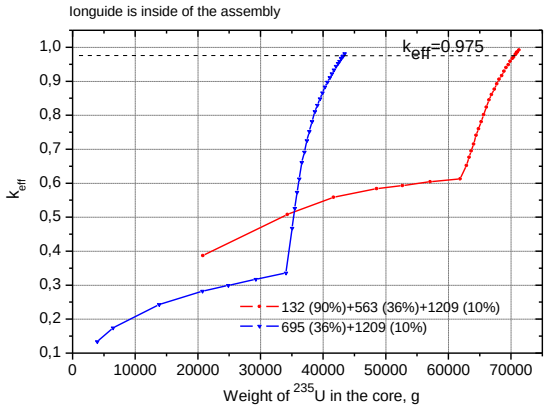

FIG. 10. Calculated k_{eff} values as a function of the loaded ^{235}U mass simulating the fuel loading steps.

The axial fission reaction rate distribution measured with Cf neutron source and the KHT-5 fission chamber is shown in Figs. 11 for the different experimental channels of this configuration.

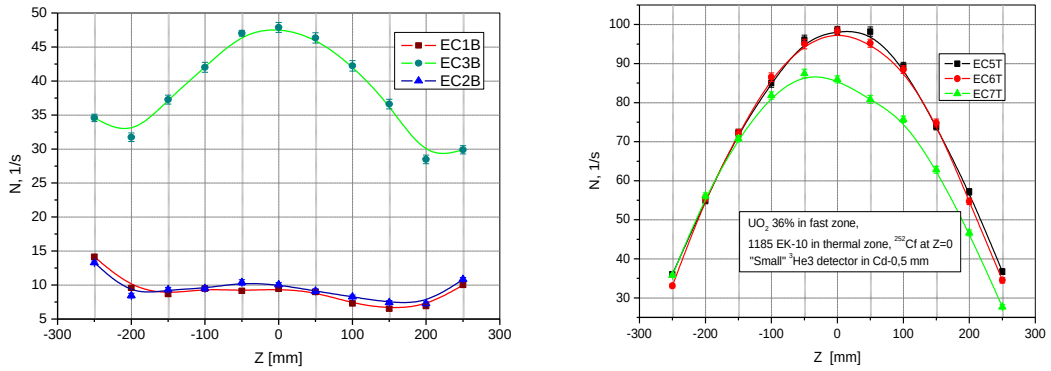

FIG. 11. Axial fission reaction rate in the experimental channels EC1B-EC3B of the fast zone and EC5T-EC7T of the thermal zone measured with ^{252}Cf neutron source of the second YALINA-Booster configuration.

The comparison of the calculated axial neutron flux distributions in the first and the second configurations calculated with Cf neutron source is given in Fig. 12. The corresponding radial neutron flux distributions calculated with D-D neutron source are shown in Fig. 13.

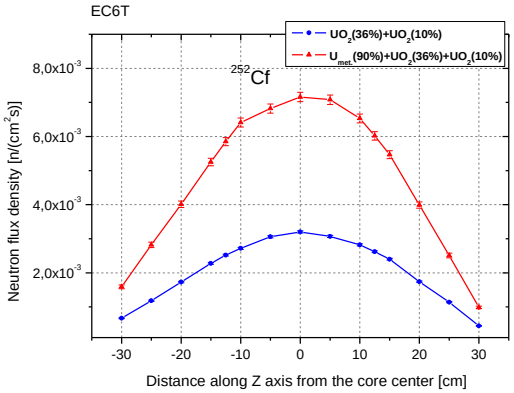

FIG. 12. Calculated axial neutron flux distributions in the experimental channel EC6T from ^{252}Cf neutron source for the first and second YALINA-Booster configurations

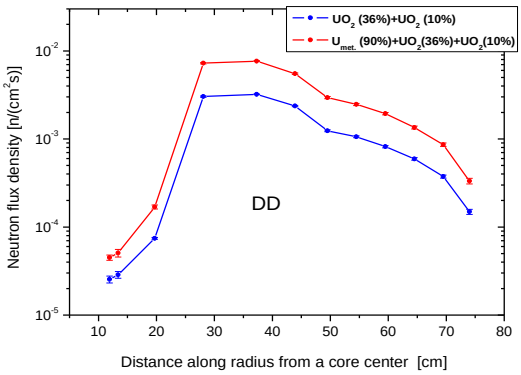

FIG. 13. Comparison of the calculated radial neutron flux distributions for the first and the second configurations.

4. NEUTRONICS PARAMETERS OF THE YALINA-BOOSTER AT THE SECOND LEU CONVERSION STEP

In this step, all the 36% enriched UO_2 fuel rods were discharged from the fast zone and replaced with 21% enriched UO_2 fuel rods and the 1185 EK-10 fuel rods were left in thermal zone. Since the available number of the 21% enriched UO_2 fuel rods is not sufficient to fill all the 695 fuel channels, 76 fuel channels were left empty. The loading procedure was simulated by MCNP calculations. The calculated k_{eff} as a function of the number of 21% enriched UO_2 fuel rods loaded into fast zone is shown in Fig. 14 for normal and accidental operating condition.

The sub-criticality level has been measured by reciprocal counting, PNS Sjöstrand, and PNS Gozani methods. The reciprocal counting numbers measured at the loading steps are depicted in Fig. 15. The third configuration contained 601 fuel rods with 21% enriched UO_2 in fast zone and 1185 EK-10 fuel rods in thermal zone.

To study the influence of neutron detector position on the sub-criticality measurements, the PNS measurements using Sjöstrand and Gozani methods were performed in all the experimental channels of the assembly. The effective neutron multiplication factor values obtained with the PNS measurements from the different experimental channels are shown in Fig. 16. In addition, the effective neutron multiplication factors as a function of the number of the 21% enriched fuels rods measured in EC5T and EC6T experimental channels are shown in Fig. 17 using Sjöstrand and Gozani methods. The results show the need for a correction methodology to remove the space and method dependence.

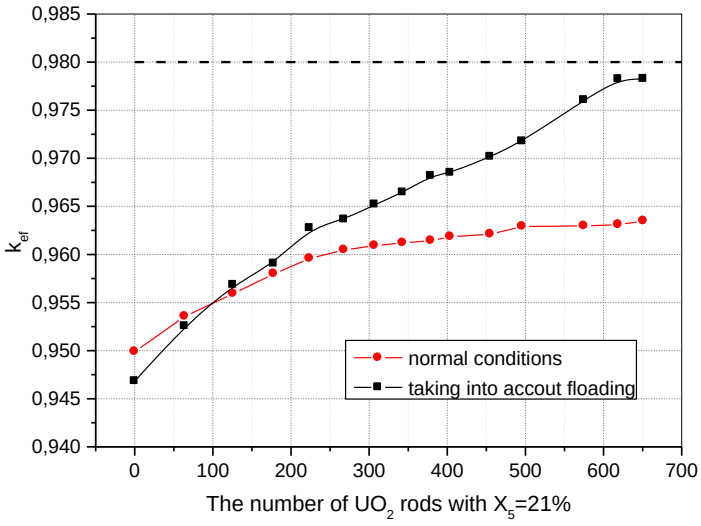

FIG. 14. Calculated effective neutron multiplication factor as a function of the number of the 21% enriched UO_2 fuel rods in the fast zone of YALINA-Booster assembly under normal and accidental operating conditions

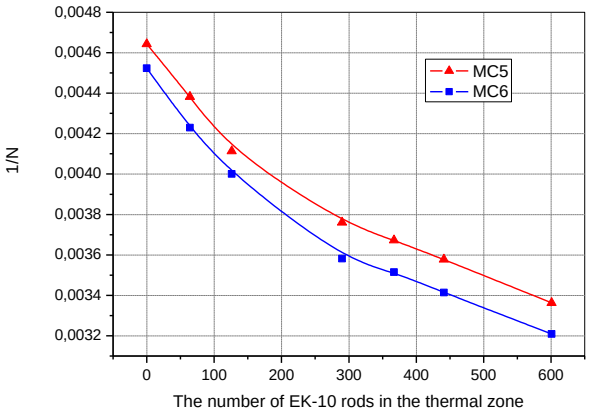

FIG. 15. Reciprocal reaction rate counting rate as a function of the number of 21% enriched UO_2 fuel rods in the fast zone and 1185 EK-10 fuel rods in thermal zone.

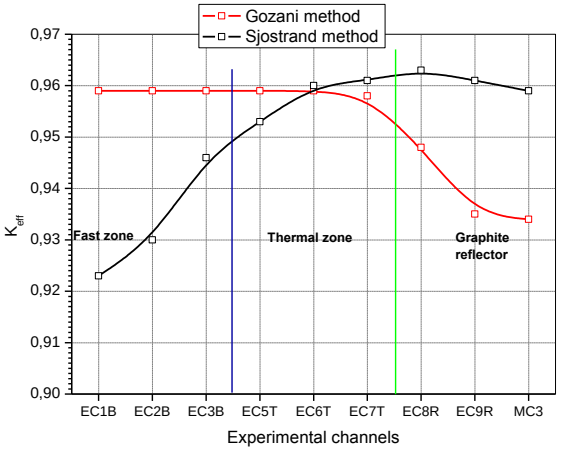

FIG. 16. Effective neutron multiplication factor estimated by PNS method using the different experimental channels, different data processing techniques, and D-D neutron source at Z=0.

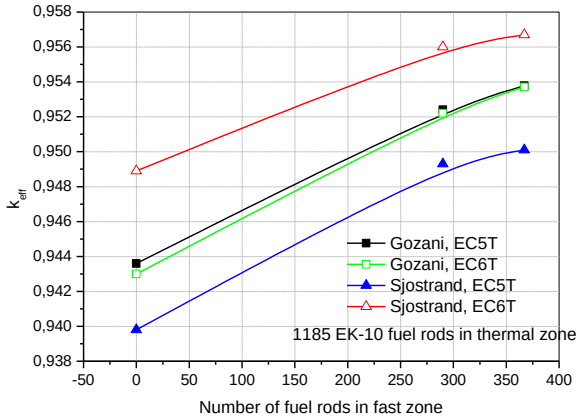

FIG. 17. Effective multiplication factor estimated by different techniques using the experimental measurements as a function of the number of fuel rods loaded into fast zone.

The neutron multiplication factor of the third configuration did not reach the 0.975 values because the number of the 21% enriched fuel rods is not sufficient. In addition, 76 fuel channels in the fast zone were empty and leaking neutrons. New configurations were developed to remedy this problem and it will be tested in the next experimental campaign.

The axial ^{3}He(n,p) reaction distribution was measured by the small ^{3}He detector in all experimental channels of the fast and the thermal zones with 50 mm steps from ^{252}Cf neutron source located at Z=0. The measured distributions are shown in Fig. 18.

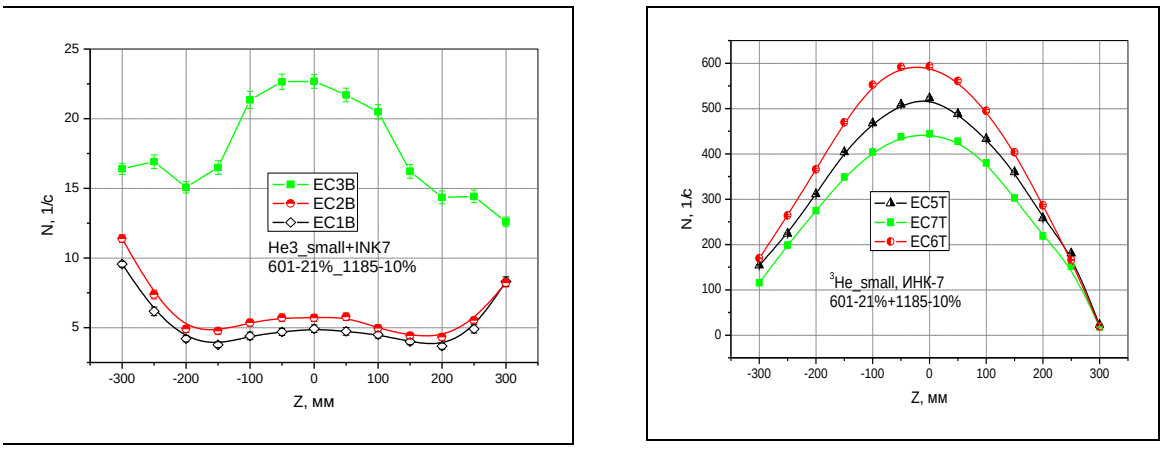

a b

FIG. 18. Axial ^{3}He(n,p) reaction distributions in the experimental channels of fast (a) and thermal zone (b) from ^{252}Cf neutron source located at the assembly center.

The comparison of the axial ^{3}He(n,p) reaction distributions in the experimental channel ECB1 of the fast zone from ^{252}Cf neutron source located the assembly center are shown in Fig 19 for the three core configurations of YALINA-Booster. The three distributions have similar shape except the scale is different. This is due to the different values of the neutron multiplication factor of these configurations.

5. CONCLUSIONS

The YALINA-Booster assembly was developed to study the neutronics of sub-critical systems driven systems with external neutron sources. The obtained experimental results from the YALINA-Booster facility provided important scientific contributions to the development of the accelerator driven systems around the world. In addition, the

experimental data are used to benchmark and validate methods and computer codes for designing and licensing ADS.

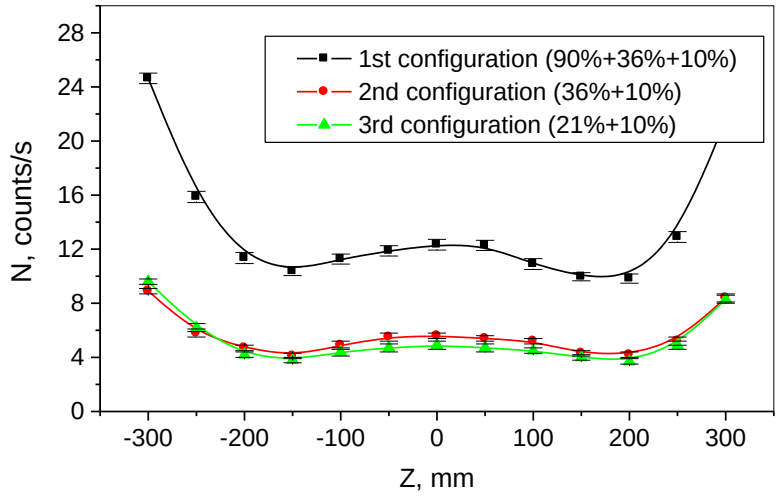

FIG. 19. Axial distribution of small size ^{3}He detector counting rate in the experimental channel ECB1 of fast zone by ^{252}Cf neutron source

YALINA-Booster studies performed during conversion of the fast zone to use low enriched uranium fuel reached the following conclusions:

— The replacement of the 90% enriched metallic uranium fuel with 36% enriched UO_2 fuel in the inner region of the fast zone requires additional 10% enriched UO_2 in the thermal zone to maintain the original k_{eff} value. The YALINA-Booster neutronics performance did not change, except for insignificant softening of the neutron spectrum in the inner region of the fast zone;

— As it was expected, the second conversion step using 21% enriched UO_2 in fast zone resulted in larger reduction in the effective multiplication factor because the number of the 21% enriched fuel rods is not sufficient. In addition, 76 fuel channels in the fast zone were empty and leaking neutrons. New configurations were developed to restore the original performance and it will be tested in the next experimental campaign. The estimated k_{eff} value from MCNP is 0.961 and the experimental value is 0.959. The corresponding values for the HEU configuration are 0.979 and 0.975, respectively;

— The Sjöstrand area ratio method predicts the subcritical assembly reactivity with high accuracy. However the method is sensitive to spatial effects caused by core heterogeneity and the detector's position relative to the external neutron source position.

REFERENCES

[1] IAEA, Working Material, Research Coordinated Meeting of the Coordinated Research Project on "Analytical and Experimental Benchmark Analyses of Accelerator Driven Systems," 5-9 Dec 2005 Minsk, Belarus, IAEA-RC-1003.1, TWG-FR/127, Vienna (2006).